

Article

# Investigation into Forming Limits of Multi-Layer Hybrid Sheets with different Materials in the Middle

Shichen Liu<sup>1</sup>, Lihui Lang<sup>2,\*</sup>, Shiwei Guan<sup>3</sup>, Sergei Alexandrov<sup>4,5</sup> and Yipan Zeng<sup>6</sup>

<sup>1</sup>School of Mechanical Engineering and Automation, Beijing University of Aeronautics and Astronautics, 100191, Beijing; liu\_shichen94@163.com

<sup>2</sup>School of Mechanical Engineering and Automation, Beijing University of Aeronautics and Astronautics, 100191, Beijing; lang@buaa.edu.cn

<sup>3</sup>School of Mechanical Engineering and Automation, Beijing University of Aeronautics and Astronautics, 100191, Beijing; gsw@buaa.edu.cn

<sup>4</sup>School of Mechanical Engineering and Automation, Beijing University of Aeronautics and Astronautics, 100191, Beijing; sergei\_alexandrov@spartak.ru

<sup>5</sup>Institute for problems in Mechanics of the Russian Academy of Sciences, Moscow 119526, Russia; sergei\_alexandrov@spartak.ru

<sup>6</sup>Chengdu Aircraft Manufacturing Company LTD, Qingyang District Chengdu, 610073, Sichuan; zengyp\_aero@163.com

\* Correspondence: liu\_shichen94@163.com; Tel.: +86 1082316821

**Abstract:** Fiber-metal laminates (FMLs) such as Kevlar reinforced aluminum laminate (ARALL), Carbon reinforced aluminum laminate (CARALL), and Glass reinforced aluminum laminate (GLARE) offer great potential for weight reduction applications in automobile and aerospace construction. In order to investigate the feasibility for utilizing such materials in the form of laminates, sheet hydro-bulging tests are studied under the condition of uniform blank holder force for three-layered aluminum and aluminum-composite laminates using orthogonal carbon and Kevlar as well as glass fiber in the middle. The experimental results validate the finite element results and they exhibited that the forming limit of glass fiber in the middle is the highest among the studied materials, while carbon fiber material performs the worst. Furthermore, the crack modes are different for the three kinds of fiber materials investigated in the research. This study provides fundamental guidance for the selection of multi-layer sheet materials in the future manufacturing field.

**Keywords:** fiber-metal laminates (FMLs); multilayer sheet bulging; forming limits; numerical simulation; crack modes

## 1. Introduction

Hybrid materials such as fiber metal laminates are being widely used in aerospace and automobile industries to replace the conventional metals and alloys for additional weight reduction, strength, and fuel economy [1]. Lightweight alloys, for instance, aluminum have lower fatigue strength and damage tolerance whereas, the composite materials like carbon fibers or glass fibers have a poor impact and residual strength. Such materials in the form of Fiber metal laminates produce a synergistic effect and offer better fatigue resistance, mechanical as well as thermal properties and improved environmental protection [2, 3, 4]. Fiber Metal Laminate (FML), as its name implies, is a type of metal materials comprising of a laminate of many thin metal layers

adhesive, bonded with the composite material layers [5, 6]. Some common commercially available FMLs include ARALL (Kevlar Reinforced Aluminum Laminate), based on Kevlar fibers, GLARE (Glass Reinforced Aluminum Laminate), based on high strength glass fibers and CARALL (Carbon Reinforced Aluminum Laminate), based on carbon fibers etc. The advent of ARALL materials is considered as the first generation fiber reinforced metal laminate aiming to make a great contribution to the lightweight design and improved fatigue resistance of the aircraft. But due to the great gap between thermal expansion coefficient of the Kevlar fiber and aluminum alloy, the great residual stress during the solidifying and cooling process was produced which made it difficult for the fabrication of large curvature components and thus restrain the applications in the aerospace and aircraft field [7]. In order to solve the problems of big residual stress and poor formability, the Fokker Company in Netherland developed the glass fiber-reinforced materials which substituted for the Kevlar fiber in the middle. Excellent fatigue strength (three times of the Aluminum 2024) and damage tolerance (increase one to two times compared with Aluminum 2024), superior impact resistance (almost 86% higher than the Aluminum 2024 of the same thickness), greater potential for weight loss (15% to 30% weight reduction than Aluminum 2024) determine the extensive application prospect of the GLARE materials in the new generation of high technology manufacturing area [8, 9]. Carbon fiber materials, a new kind of high-strength fiber applied in the third generation of fiber metal laminates which possess the outstanding mechanical properties still need to be further research for the commercialized production. In fact, the existence of potential difference makes the electrochemical corrosion occurs between the interlayers which seriously affected the fatigue characteristics of the laminate materials [10, 11, 12].

In general, the traditional approach to measuring the relationship between stress and strain, as well as the forming limits of the fiber metal laminate sheet, is the unidirectional tensile test of the blank materials. For example, G.R. Rajkumar et al.[13] had investigated the effect of strain rate and lay-up configuration on the tensile behavior of four combinations of fiber metal laminates. He found that the tensile strength increased with the increasing strain rate and the strength were maximum for carbon-based FML structures, minimum for glass-based FML and hybrid FML material lies between them. Ankush P. et al.[14] had found from the tensile test of the glass fiber-reinforced metal laminates that the lay-up sequence had no influence on the initial modulus of the FMLs, but the ultimate strength and post-ultimate strength behavior were significantly affected by it, analyzed by the numerical simulation and experimental phenomenon. However, this kind of method mainly makes it deform on the laminate plane surface and prone to produce the phenomenon of instability. In one hand, the tensile test restrains the total deformation that can be reached by the sheet material. On the other hand, the necking effect and section distortion of the specimen induce the lateral stress which leads to the inconsistent with the axial stress ( $\sigma_1$ ) and yield stress ( $\sigma_s$ ),  $\sigma_1 > \sigma_s$ . Moreover, the uneven distribution of  $\sigma_1$  along the specimen section causes relatively large errors if we still regard  $\sigma_1 = \frac{P}{A}$  as the axial stress.

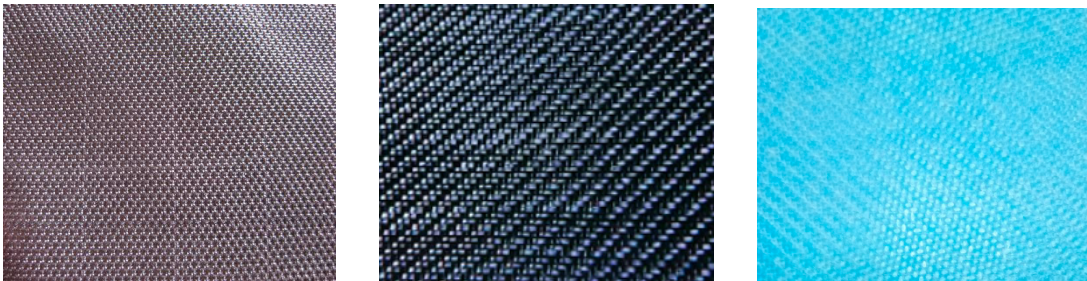
In order to solve the above-mentioned problems, it has been widely used to apply hydraulic bulging test to obtain the mechanical behavior of the sheet materials. Correia J P M et al.[15] adopted the method of finite element modeling to conduct the electromagnetic sheet bulging test which has the advantages of improved formability, high productivity and reduction in tooling cost. Wang Z et al.[16] put forward the ductile fracture criterion to find the forming limits of aluminum alloy

6k21-T4 sheet by bulging process in both simulation and experimental tests. He Z et al. [17] has studied the mechanical properties of tubular materials through analyzing the tube hydro-bulging experiments and proved it more feasible in characterizing the deformation behavior under bi-axial stress state. Wang Y et al.[18] presents the overlapped sheet hydraulic bulge test which can improve the formability of low plasticity metal by controlling the force conditions and stress states of target sheets. In our study, the same measurement method of the forming limits of the multilayer composite sheet by the hydro-bulging test has been adopted to verify its formability.

2. Materials and Methods

2.1 Materials

The material of upper and lower layer of the 2/1 multilayer hybrid sheet is aluminum alloy 2024-O with the thickness of 0.4 mm. The material properties along the three main rolling directions are shown in Table 1. In order to compare the formability of the multilayer sheet by measuring the forming limits in the hydraulic bulging test, different cross-ply fibers including carbon, Kevlar and glass(shown in Fig.1 ) as well as the same kind of aluminum alloy with uniform thickness( $t = 0.2\text{ mm}$ ) are carried out respectively. The blank size of the multilayer sheet is 150 mm  $\times$  150 mm and the method of constructing the composite laminate (apply the epoxy resin to the fabric) is known as dry layup where the coefficient of contact friction is small. Elastic properties of different material constituents in the laminate are shown in Table 2. The low plasticity of composite material which can be neglected in the test varies greatly in the forming behavior of the aluminum alloy 2024-O. Value of these parameters is consistent to make a good agreement on the experimental results and finite element simulation analysis.



(a) Kevlar fiber (b) Carbon fiber (c) Glass fiber  
Fig.1. Different kind of fiber materials in the middle used in the experimental test

Table 1. Material Parameter of Sheet Al 2024-O

Blank material	Rolling directions(°)	Yield stress/MPa	Ultimate strength/MPa	Anisotropy Factor $R$	Strain hardening exponent
Al 2024-O	0	63.9	180.8	0.783	0.195
	45	58.1	170.4	0.823	0.184
	90	59.1	169.1	1.1	0.191

111

Table 2. Elastic properties of different material constituents in the laminate

Material	Density ( $g / cm^3$ )	$E_1$ ( $GPa$ )	$E_2$ ( $GPa$ )	$V_{12}$	$G_{12}$ ( $GPa$ )	$G_{23}$ ( $GPa$ )	$G_{13}$ ( $GPa$ )
Al 2024-O	2.72	73.1	73.1	0.33	28.0	28.0	28.0
Carbon Fiber/Epoxy	1.76	232.0	8.61	0.28	3.75	2.30	2.30
Kevlar Fiber/Epoxy	1.44	85.3	5.5	0.4	2.54	0.97	0.97
Glass Fiber/Epoxy	2.52	53.98	9.412	0.23	3.50	2.06	2.06

112

113

2.2 Experiment

114

Fig.2 schematically illustrates the multilayer sheet hydraulic bulging test procedure researched

115

in the study. The flange of the external sheet is in contact with the lower die and necessary blank

116

holder force is provided by the upper die. The laminated blank gradually deforms with the increase

117

of the cavity bulging pressure affected on the bottom of the sheet. The hydraulic bulging equipment

118

is applied to test the forming limits of three kinds of fibers as well as the conventional aluminum

119

alloy in the middle and the diameter of the liquid chamber is 80 mm. The tests were conducted on

120

the self-developed 500KN sheet hydroforming machine at Beihang University which was controlled

121

by a hydraulic feed device connecting to the software installed in the computer shown in Fig.3. The

122

cavity pressure increases smoothly and stops immediately as the laminate cracks reaching its limits

123

during the bulging procedure. Values of the maximum cavity pressure and the limit bulging height

124

can be recorded immediately from the computer screen. Ultrasonic testing (UT) was utilized to

125

evaluate the wall thickness distribution in individual layers coupled with the limit bulging height

126

when the multilayer hybrid sheet fractures. Also, the friction coefficients between the interlayers

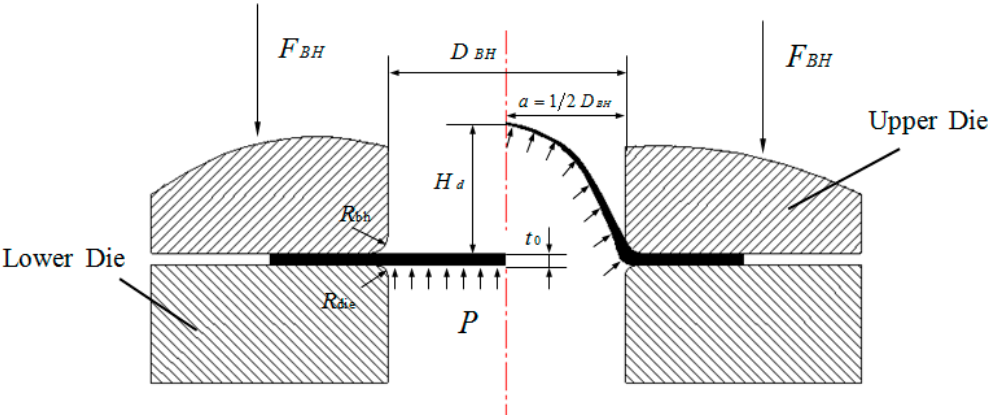
127

and testing moulds used in the finite element simulation analysis were measured by the friction

128

equipment detection machine MXD-02 following the ISO standard ASTM D1894.

129



130

131

Fig.2. Schematic diagram of multilayer sheet hydraulic bulging process

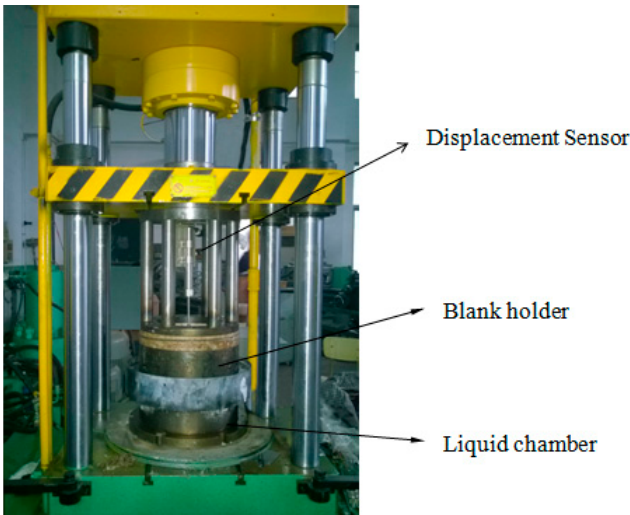


Fig.3. Multi-layer sheet hydro-bulging test machine

2.3 Finite element method model

Finite element analysis software ABAQUS/Explicit was used in measuring the forming limits of the multilayer sheet. The numerical simulation model is represented in Fig.4 where the mold size and process parameter are the same as the experimental test including liquid chamber cavity dimension (80 mm) and the fixed blank holder force (20KN). Elastic and plastic properties of the aluminum alloy, as well as the engineering constants and expansion factor of the composite fibers, were imported into the material property module of the software. Also, the Hashin damage criterion inside the software was used in predicting the initial fracture moments. Blank holder and the liquid chamber were considered as discrete rigid with a mesh size of 5 and the laminate sheet set as a 4-node doubly curved shell with reduced integration was treated as deformable bodies meshing a size of 4. Fiber orientation can also be established as cross-ply ( $0^{\circ}/90^{\circ}$ ) direction in the finite element simulation analysis. A friction coefficient of 0.05 was used for the interfaces between the outer metal layer and the middle layer, and 0.12 for that between the upper metal sheet and the blank holder, 0.1 for that between the lower metal sheet and the liquid chamber, respectively.

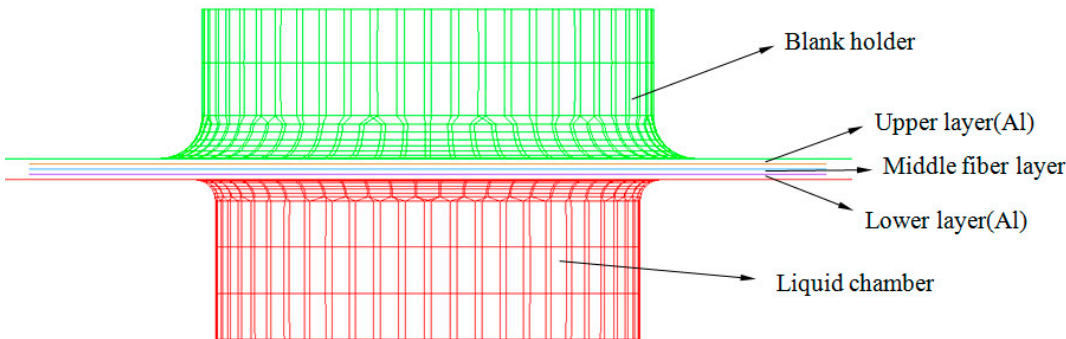


Fig.3. Finite element method model of the three-layer sheet bulging process



### 3. Results and discussion

#### 3.1 Maximum cavity pressure and limit bulging height

As can be seen from the experimental results, shown in Fig 4, that the crack phenomenon all occurred around the curvature peak area where the laminate central region located and the forming limits are measured to be different due to the various materials tested in the middle. During the hydraulic bulging procedure, bulging height gradually raise as the increase in the pressure of the fluid chamber and dropped immediately when the sheet laminate approaches the critical point of instability which finally result in a large crack. The two index parameters (limit bulging height and maximum cavity pressure) evaluating the forming limits measured by experiment and numerical simulation are represented in Fig 5 and 6. Fig.5 indicates that the limit bulging height is 17.1 mm in the experimental test when the aluminum sheet is used in the middle of the laminate. However, the synergistic effects are diverse with different fibers substituting the metal sheet in the middle. As for the Kevlar and glass fiber tested in the experiment, the limit bulging heights are 20.3 mm and 25.2 mm respectively, 18.7% and 47.4% improvement in formability. But the effect is negative for the carbon fiber in the middle which measured only 15.8 mm height to the bulging limit, and the reduction rate is about 7.6%. Similarly, the comparative relation is the same for the maximum cavity pressure shown in Fig.6 in the hydro-bulging experiment. The maximum pressure effect by the fluid chamber for the multilayered aluminum sheet is 13.8 MPa and the maximum cavity pressure decrease to 12.6 MPa for the carbon fiber in the middle. It is also obvious to see that for Kevlar and glass fiber replacing the aluminum alloy and carbon, the combined effects are positive with 14.3 MPa and 17.8 MPa for the maximum cavity pressure, respectively. By comparing the results from the above figures, it is easy to conclude that the forming limit for glass fiber in the middle of the three-layer sheet is the highest which also demonstrate the formability is the best, followed by the better forming behavior for Kevlar fiber, and the carbon fiber having inferior limit height coupled with maximum pressure and formability among the four kinds of materials tested in the laminate middle. Finite element simulation results reveal a high degree of consistence with the experimental ones within reasonable errors.

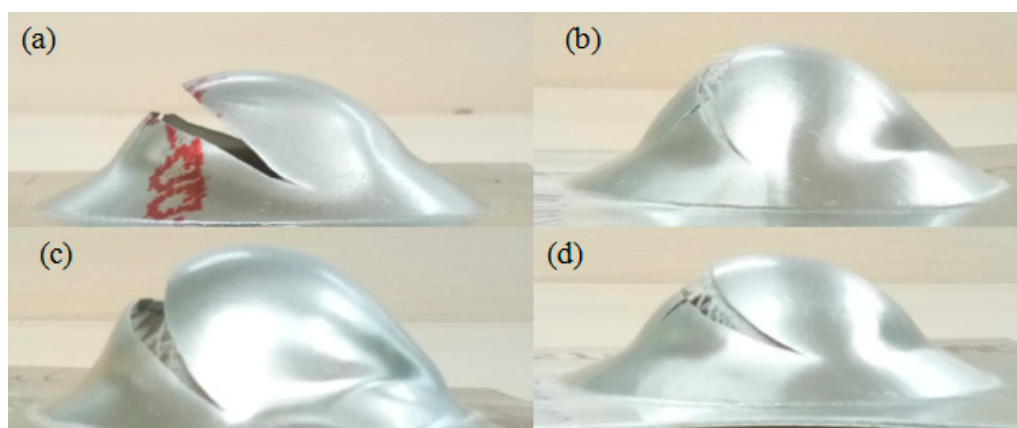


**Fig.4.** Experimental results comparing different materials in the middle of the laminate:

(a) Aluminum sheet    (b) Kevlar fiber    (c) Glass fiber    (d) Carbon fiber

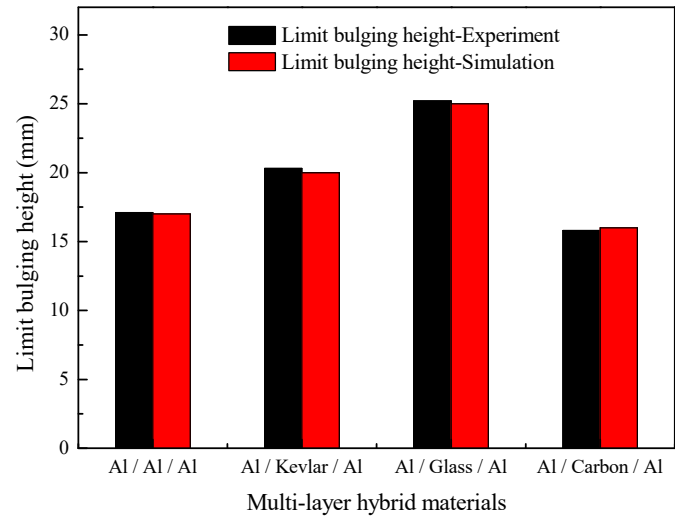


Fig.5. Limit bulging height of test laminates with different materials in the middle

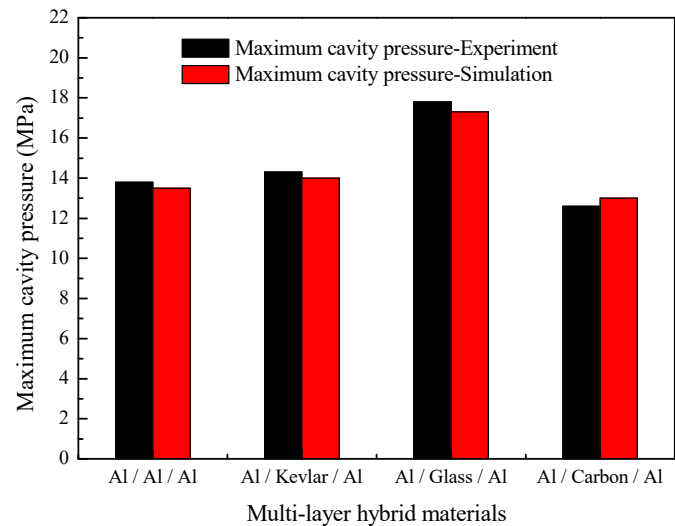


Fig.6. Maximum cavity pressure of test laminates with different materials in the middle

3.2 Stress-strain and wall thickness distribution

In order to study deeply on the forming limits and formability of the multilayer sheet especially the materials in the middle, the paper works on the stress-strain and wall thickness distribution of the tested materials at the instant of the crack phenomenon occurs. It is the fundamental analysis to research on sheet deformation mechanisms which also provides an innovative judgment of the crack modes for different fibers in the middle discussed in next section. In the finite element simulation model, it can be regarded as the normal direction (0°) for the rolling direction of aluminum alloy and also one of the principal orientations for the fiber materials. Fig.7 represents the stress distribution of different materials in the middle along this direction ( $S_{11}$ ). The results indicate that the maximum stress occurs at the central region which undergoes the maximum deformation for all the studied

materials and the variation of stresses differs significantly for the aluminum alloy and fiber materials due to the differences between cross-ply composites and the approximately isotropic property of the metals along rolling direction. It is also obvious to obtain from the stress distribution diagram that the stress for the aluminum sheet in the middle is much higher than the fiber materials. Nevertheless, the edge of the fiber materials produces a remarkable deformation in contrast to the aluminum alloy on account of the limited plasticity of the above composite. For the different fiber composites in the middle, although there is not much distinction in stress distribution, the details for the comparison with the three fiber performance are well investigated. Carbon fiber in the middle experience the maximum stress at the crack moment along the principal direction, glass fiber follows and Kevlar fiber is the least among them. The reason why the stress distribution order is marked distinguishing compared with the limit bulging height and maximum cavity pressure discussed in the previous section is mainly due to the elastic properties especially the tensile modulus of the fibers play the leading role in the whole bulging process. Even though the forming limit for the carbon is the minimum among the studied fibers, the better capacity in elasticity makes the maximum stress along the principal direction for the carbon the highest. Stress distribution of the fiber materials in the middle, along the orientation perpendicular to the main direction ( $S_{22}$ ) is almost the same due to the pattern of orthogonal layering.

Metal or alloys have much greater failure strain normally in the range of 10-50 % while composite materials have quite limited formability as compared with the metals. The fibers fail at much fewer strain values which are around 1% for carbon fibers, 2-2.5 % for Kevlar fibers and 4-5 % for glass fibers. Numerical simulation result which measures the strain distributions of different materials in the middle along radial and circumferential direction are shown in Fig.8. Zero coordination position of the horizontal axis denotes the central location of the sheet and the symmetrical characteristic makes it possible to plot the variation curve on one side. As can be seen, the material performances have a great influence on the strain distribution of bulging specimen, the radial strain for the aluminum sheet in the middle is much greater than composite fibers due to the good plasticity which leads to the better flowability of the material. However, the maximal value of

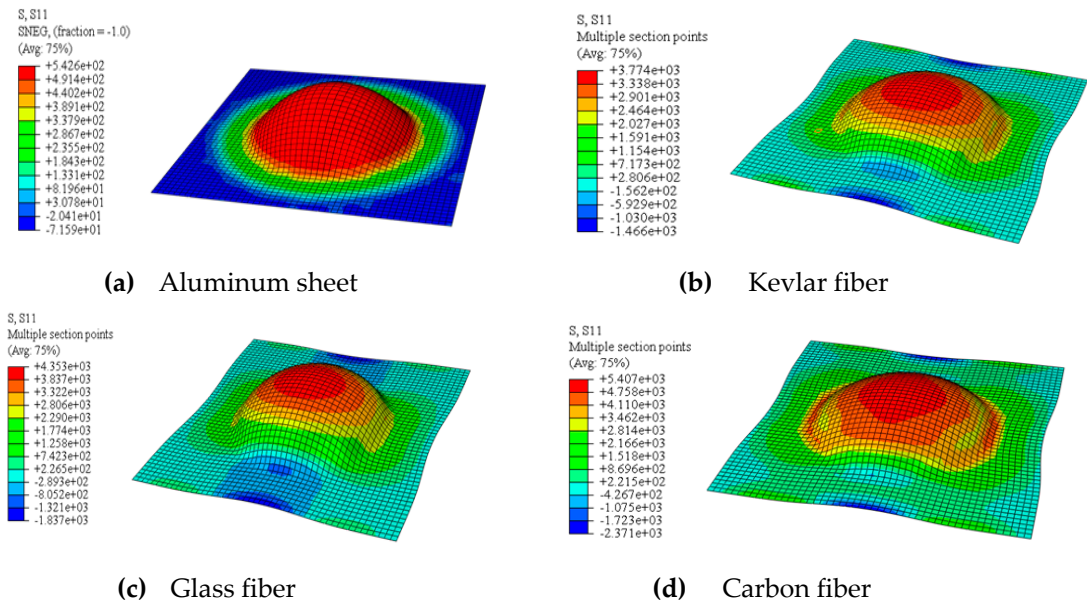
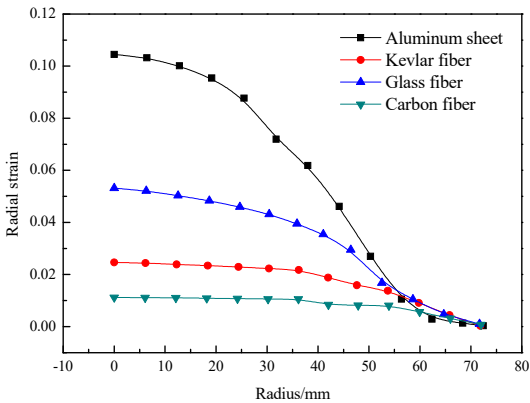


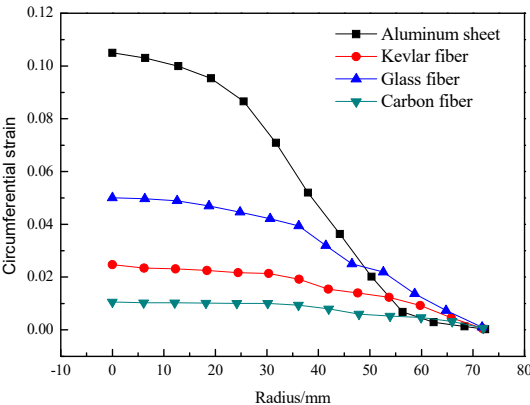
Fig.7. Stress distribution of different materials in the middle along the normal direction ( $S_{11}$ )



strain and the distribution curve uniformity along the radial direction can be dramatically improved by utilizing the glass fiber material as the middle layer when comparing the three composite fibers in the study. This is caused by the failure strain of different fiber materials displayed above. Therefore, with the selection of the glass fiber with greater failure strain and high strength, the reverse compressive stress effected on the outer aluminum sheet increases and the three-dimensional stress state enhances significantly. Also, the excessive local deformation of the multilayer sheet in the central area is limited with decreased radial and circumferential strain and the fibers are easily undergone the tensile failure during the bulging process even though the tensile modulus is not the largest among them. Thus, the forming limits for the glass fiber are the best and the formability will enhance greatly using this material. Wall thickness distributions of the materials in the middle comparing experiment and finite element modeling results represented in Fig.9 are also a key factor that influences the forming behavior of the sheet, particularly for the aluminum alloys. The picture clearly demonstrates that there is almost no wall thickness reduction for the carbon fiber owing to the lesser failure strain of such material, which results in the minimum bulging height at the same time. But the aluminum sheet can bear more thickness reduction because of the unique material mobility of the metals in comparison to the composite fibers. The maximum thinning rate in the test can reach to 15.2 % while the value is 15.8% compared with numerical simulation results.



(a) Radial strain



(b) Circumferential strain

Fig.8. Strain distribution of different materials along radial and circumferential direction

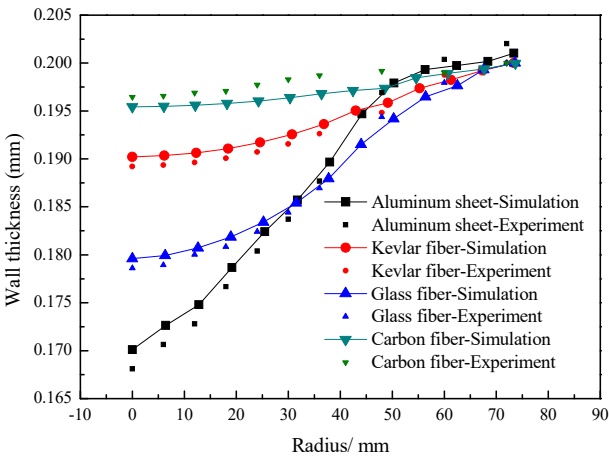


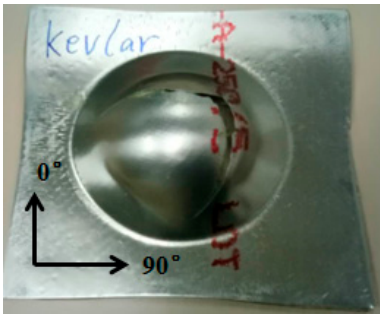
Fig.9. Wall thickness distributions of different materials in the middle

3.3 Fracture criterion and crack modes

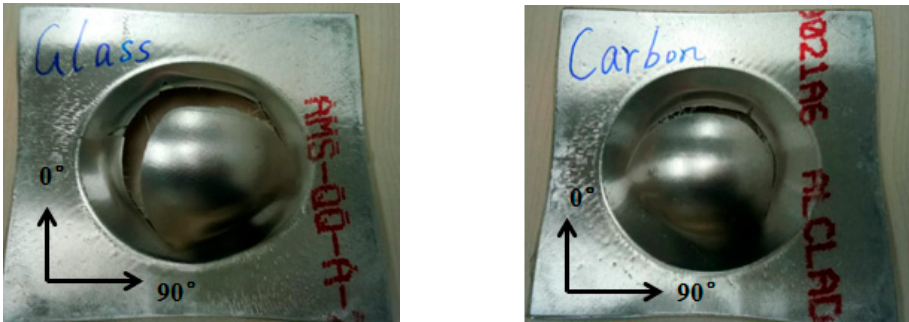
Fig.10 exhibits the geometrical profile of the crack bulging part using the aluminum sheet and three kinds of fiber in the middle. Comparing the fracture mode of the metal and cross-ply fibers, it is obvious to see that the three-layer aluminum sheet cracks along a certain orientation following the rolling direction, but the multilayer blank fracture orthogonally ( $0^{\circ}/90^{\circ}$ ) for the three fibers in the middle on account of the pattern of orthogonal layering. To investigate more about the crack mode of the fiber metal laminates, it is critical to judging the deformation of the outer aluminum layer and middle layer which fracture first during the bulging process. Even though the experimental result may be slightly hard to reflect the phenomenon and then measure the failure criterion, it is evident to get the detailed conclusion from every reprocessing step in finite element modeling analysis. According to the forming limit diagram (FLD) of the aluminum 2024-O and the failure strain of the used fiber materials, the middle layer has been deduced to fracture first and the outer aluminum layers fail at the same time even though they have not reached the forming limits. Fig. 11 reflects the maximal thinning rate of the upper aluminum layer which undergoes the maximum deformation at the initial moment of cracking. The result explains exactly why the glass fiber in the middle exhibits the best formability while carbon fiber shows the worst forming limits. The lowest thickness reduction of the outer layer at the instant of fracture demonstrates that the multilayer cracks quickly without performing the outstanding elastic-plastic properties and excellent forming behavior of the aluminum alloy when the carbon lay up in the middle. As for the glass fiber, the three-layer sheet



(a) Aluminum sheet



(b) Kevlar fiber



(c) Glass fiber (d) Carbon fiber

**Fig.10.** Geometrical profile of the crack bulging part comparing four different materials in the middle.

fails almost simultaneously with the metal and fiber material reaching the forming limits. This kind of fracture modes provide a basic guidance for the future selection of fiber metal laminates and prove that glass fiber in the middle which can also be called as GLARE materials have a wide application in the manufacturing area.

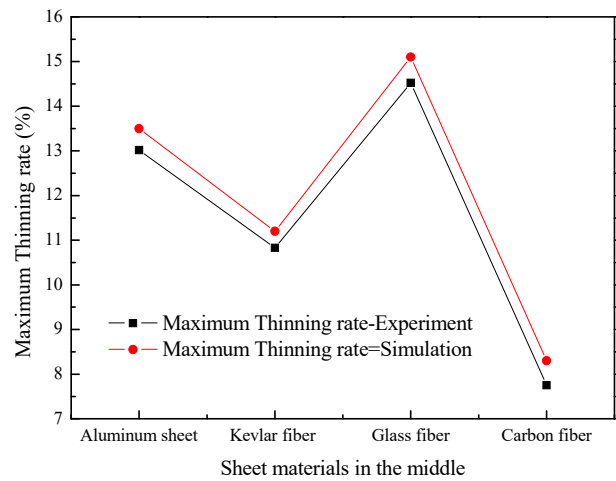


**Fig.11.** Maximum thinning rate of the upper aluminum layer at the instant of cracking

**5. Conclusions**

- (1) Compared with the three-layer aluminum sheet hydro-bulging process, the fiber material substituting in the middle have distinct influence on the forming limit measured by the limit bulging height and maximum cavity pressure. Glass and Kevlar fiber used in the study is more conducive to the improvement of multilayer sheet formability while carbon fiber has little or even no impact.
- (2) There is a big difference in stress-strain and wall thickness distribution of aluminum alloy and different fiber materials in the middle of the multilayer sheet. Among the studied factors, failure strain of the fibers as well as the thickness reduction rate of the aluminum sheet play a key role in the formability of this kind of three-layer blank while the fracture mode which explains the sequence of crack layers at the instant of fracture well validate the distinction between the researched materials.

- (3) For commercial-scale production, the formability of multilayer sheet can be greatly improved by using the glass fiber in the middle. The relatively large forming limit and better formability of the material in the hydro-bulging process makes it easy to form the specific part and the comprehensive performance coupled with lightweight features illustrate the reason why the GLARE materials have extensive applications in the aircraft manufacturing field.

**Acknowledgments:** The authors greatly acknowledge the financial support from National Science and Technology Major Project with Grant No.2014ZX04002041 and National Science Foundation of China with Grant No.51675029.

**Conflicts of Interest:** The authors declare that they have no conflict of interest.

## References

1. Botelho, E.C. A review on the development and properties of continuous fiber/epoxy/aluminum hybrid composites for aircraft structures. *Materials Research*, **2006**; 9: 247-256
2. Vogelesang L.B; A. Vlot. Development of fibre metal laminates for advanced aerospace structures. *Journal of Materials Processing Technology*, **2000**; 103(1): 1-5
3. A.J.R Vermeeren. A Historical Overview of the Development of Fiber-metal Laminate. *J Composite Material*, **2003**; 10: 189-205
4. Asundi A; Choi AYN. Fiber metal laminates: An advanced material for future aircraft. *J Mater Process Tech*, **1997**; 63: 384-394
5. G. Reyes, H. Kang. Mechanical behavior of lightweight thermoplastic fiber-metal laminates. *J Mater Process Tech*, **2007**; 186: 284-290
6. Olga Sokolova; Adele Carrado; Heinz Palkowski. Metal-polymer-metal sandwiches with local metal reinforcements: A study on formability by deep drawing and bending. *Composite Structures*, **2011**; 94 : 1-7
7. Vogelesang, L.B; Gunnink, J.W. ARALL: A materials challenge for the next generation of aircraft. *J. Mater. Design*, **1986**; 7:287-300
8. Guocai Wu; J-M Yang. The Mechanical Behavior of GLARE Laminates for Aircraft Structures. *J Failure in Structural Materials*, **2005**;7:72-79
9. Sang Yoon Park; Won Jong Choi ;Heung Soap Choi .A comparative study on the properties of GLARE laminates cured by autoclave and autoclave consolidation followed by oven postcuring. *Int J Adv Manuf Technol*, **2010**; 49:605-613
10. Yanagimoto J; Ikeuchi K. Sheet forming process of carbon fiber reinforced plastics for lightweight parts. *J CIRP Annals-Manufacturing Technol*, **2012**; 61 (1): 247-250
11. Díaz, J. and L. Rubio. Developments to manufacture structural aeronautical parts in carbon fibre reinforced thermoplastic materials. *Journal of Materials Processing Technology*, **2003**; 43-144(0): 342-346
12. Hou, M; L. Ye; Y.W. Mai. Manufacturing process and mechanical properties of thermoplastic composite components. *Journal of Materials Processing Technology*, **1997**; 63(1-3): 334-338
13. G.R. Rajkumar; M. Krishna. Investigation of tensile and bending behavior of aluminum based hybrid fiber metal laminates. *Procedia Materials Science*, **2014**; 5:60-68

- 336 14. Aukush.P; Sanan H. Experimental and numerical investigation on the uniaxial tensile response and failure  
337 of fiber metal laminates. Composites Part B, **2017**; 125(15):259-274
- 338 15. Correia J P ; Ahzi S. Electromagnetic Sheet Bulging: Analysis of Process Parameters by FE Simulations.  
339 Key Engineering Materials, **2013**; 554: 741-748.
- 340 16. Wang Z J, Li Y. Evaluation of forming limit in viscous pressure forming of automobile aluminum alloy  
341 6k21-T4 sheet. Trans Nonferrous Met Soc China, **2007**; 17:1169-1174.
- 342 17. He Z B; Yuan S J. Analytical model for tube hydro-bulging tests, part II : Linear model for pole thickness  
343 and its application. International Journal of Mechanical Science, **2014**; 87 :307-315.
- 344 18. Yao Wang; Lihui Lang; Rizwan Zafar. Investigation into the overlapping sheet hydraulic bulge and its  
345 formability. J Braz Soc.Mech.Sci.Eng , **2016**; 38(6):1635-1645